

Exact electron spectra in collisions of two zero-range potentials with nonzero impact parameters

S. Yu. Ovchinnikov,* D. B. Khrebtukov,† and J. H. Macek

Department of Physics and Astronomy, University of Tennessee, Knoxville, Tennessee 37996-1501
and Oak Ridge National Laboratory, Post Office Box 2009, Oak Ridge, Tennessee 37831

(Received 17 October 2001; published 26 February 2002)

The Sturmian theory of ion-atom collisions is constructed for arbitrary (nonzero) impact parameters. The approach is essentially nonperturbative, and has a wide range of applicability: from low velocities, provided that quantum motion of heavy particles can be neglected, to high velocities, as long as the relativistic effects are not important. The theory is applied to calculation of electron spectra at low and high collision velocities. For slow collisions we describe Fermi oscillations in the spectra of ejected electrons. At higher velocities our theory confirms the possibility of cusp formation even when the heavy particles are neutral in the final state.

DOI: 10.1103/PhysRevA.65.032722

PACS number(s): 34.80.Dp, 34.20.Mq, 34.10.+x, 34.50.Fa

I. INTRODUCTION

In recent years, the novel technique of cold-target recoil-ion momentum spectroscopy (COLTRIMS) has allowed experimentalists to map out the full momentum distributions of ejected electrons [1]. The large amounts of data from COLTRIMS experiments present a challenge for atomic theories. For several reasons ion-atom and atom-atom collisions are notoriously difficult to describe exactly in quantum mechanics. Probably the most important conceptual difficulty is connected with the essential time dependence of collision processes, where initial conditions are set up at $t \rightarrow -\infty$, but solutions are usually needed at $t \rightarrow +\infty$. Thus, in principle, complete solutions for all values of a time variable are required.

In this paper we consider only collisions involving one-electron transitions. There are two principal methods to obtain *exact* solutions to this problem: (i) direct numerical solution in three-dimensional (3D)+time by discretization of the Schrödinger equation in a finite box [2–4] and (ii) expansion over basis sets [5]. We do not consider any perturbation theories in this paper. Difficulties of the direct numerical method are mainly due to the necessity to keep the box finite, while physical initial and boundary conditions require extension of the box to infinity. This approach is completely out of the scope of this paper and will not be discussed further.

Successful application of basis set expansion techniques depends primarily on the kind of basis functions used. The bases can be divided into two broad categories by their configurational properties: atomic and molecular. Atomic bases [6] provide a good description of inelastic processes that occur at large internuclear distances. However, the approach breaks down at smaller internuclear distances because atomic bases cannot describe the quasimolecular topology of the electronic motion [7]. Notwithstanding many creative efforts to remedy this situation [8], the expansion over atomic bases cannot provide exact solutions in a wide range of collision

parameters (relative velocities and impact parameters) without introducing *ad hoc* parameters. It should be noted, however, that the initial conditions are easy to set up in these bases, and the asymptotic translational motion of the electron can be accurately described.

The situation is reversed in case of molecular bases. They provide the best description of the electronic motion topology but it is difficult to make them Galilean invariant and to account for the translational motion of electrons with the nuclei at $t \rightarrow -\infty$, i.e., to satisfy correct physical initial conditions. This problem was recognized as early as in 1958 by Bates and McCarroll [9], and since then there were numerous (more or less successful) attempts [10] to correct this situation by appending *ad hoc* electron translation factors (ETF) to molecular functions.

A rigorous way to make molecular bases asymptotically Galilean invariant has been found by Solov'ev and Vinitisky [11]. They proposed a time-dependent scaling of the spatial variables $\mathbf{q} = \mathbf{r}/R(t)$ and an additional transformation of wave functions to preserve the form of the Schrödinger equation. While essentially solving the translational problems, the Solov'ev-Vinitisky scale transformation still does not address another drawback of the *adiabatic* molecular bases; namely, it is difficult to describe the interaction with the continuum, especially when one of the adiabatic energy curves crosses the ionization threshold. In terms of the close-coupling method it means that one of the coupled differential equations disappears at some moment of time, since the number of bound states is decreased by one [12]. Another example is the crossing of the Rydberg spectrum by a superpromotion: to reach the continuum one has to take into account an infinite number of interaction regions. These difficulties practically precluded reliable theoretical studies of the ionization processes in ion-atom collisions by using molecular bases.

The solution to this problem was found in a novel use of Sturmian molecular bases [13]. The main innovation is the integration over an energy parameter ω . Since ω is *not* an eigenvalue in the Sturmian case, the integration can be extended over both discrete ($\text{Re } \omega < 0$) and continuous ($\text{Re } \omega > 0$) parts of the Schrödinger equation's spectrum. Thus, every Sturmian function carries information about transitions between discrete levels (excitation) as well as about ionization. It follows that the convergence of such a technique is

*Permanent address: Ioffe Physical Technical Institute, St. Petersburg, Russia.

†Present address: CromoGraphics, San Francisco.

expected to be very good. Indeed, in some special cases, it is possible to obtain *exact* results by using a finite (and small) number of Sturmian functions. For instance, just one Sturmian function will be sufficient to obtain exact solutions in this paper.

The theory employing H_2^+ “molecular” Sturmian functions has already been successfully used to calculate electron spectra in proton–hydrogen atom collisions at impact parameter $b=0$ [14]. This special case offers a degree of symmetry not present at $b \neq 0$ and also employs Sturmian functions that are closely related to the more familiar H_2^+ adiabatic eigenfunctions. These circumstances allowed for a rapidly convergent calculation of electron distributions so that essentially exact results for proton-hydrogen collisions at $b=0$ were obtained.

In this paper we take the next major step by using the theory for $b \neq 0$. For sufficiently large b the cores do not interpenetrate and one can model the dynamics of the “active” electron by using only the wave function well outside the core. When the wavelength of the electron’s de Broglie wave is much larger than the dimension of the core then one can use a model where the radius of the core shrinks to a point. This is the zero-range-potential (ZRP) model [15] discussed in Sec. II A. In this model only s -wave interaction are present and they are described by the s -wave scattering length a . We consider the model of two zero-range potentials moving along a straight-line trajectory. This model has been used to study rearrangement and ionization [16,17], but their solutions have always been restricted to impact parameters $b=0$. This is a fundamental defect, since physical processes at $b=0$ involve the interpenetration of atomic cores where the zero-range assumption is invalid.

The ZRP model has several features that make it amenable to the molecular Sturmian theory. Most important, there is only one Sturmian function and a closed-form expression for it has been found [19]. Because there is no need to truncate an infinite series, an exact solution is possible. In this paper we find the exact solution for this model problem and study the effect that nonzero impact parameters have on the electron distributions in the process

$$A^- + A \rightarrow A + A + e^-, \quad (1)$$

where the electron-atom interaction is modeled by the s -wave scattering phase shift

$$k \cot \delta = -1/a, \quad (2)$$

with constant scattering length a .

The theory is built along the general lines presented in our previous paper [13] (Secs. III A and III B). However, the relative simplicity of the ZRP case allows us to analyze in detail the crucially important problem of the initial conditions (Sec. III C). It is not trivial to satisfy initial conditions in this theory because the solution is actually carried out in Fourier space (ω space) while the initial conditions must be set up in the physical time space (t space). It has been shown already [13] that ω and t space can be connected by the stationary-phase approximation at $t \rightarrow -\infty$. In Sec. III C we

show that two more considerations should be taken into account while dealing with the initial conditions. First, the Fourier integral must converge which requires a solution in ω space that would decrease at large positive $\text{Re } \omega$. Second, the stationary-phase approximation of the exact solution in t space must coincide with the stationary-phase approximation of the initial conditions. This allows us to find the unique solution to the problem. Although our solution uses only one molecular Sturmian wave function it is exact even for high collision velocities [18]. This emphasizes the difference between molecular Sturmian functions and adiabatic bases.

We construct a theory that has an extraordinarily wide range of validity in terms of collision energy: from thermal energies, as long as we can neglect quantum motion of nuclei, up to high energies provided that relativistic effects are not significant yet. The theory is mathematically exact, i.e., we do not use or imply any approximations. Therefore, the results of calculations presented in Sec. V can be used as reference data for other theoretical methods and, if the physical conditions of validity are satisfied, i.e., s -wave dominance in electron-atom scattering, they can be used to describe experimental data. To illustrate the wide range of our theory we show cusp and binary encounter peaks in the spectra at high energies. Our calculations confirm the possibility of cusp formation when heavy particles (atoms) are neutral in the final state [20]. We did not see a pronounced interference between gerade and ungerade amplitudes, called Fermi oscillations [21], in the electron spectra at low collision velocity (adiabatic regime) when the impact parameter $b \neq 0$, that were found for $b=0$ [17]. Our calculations are compared with hidden crossing results at low collision velocity. Note, that in ZRP model the electron spectra at low collision velocity is different from the spectra of collisions of positive ions with atoms, where the saddle-point electrons dominate. In this model there are no saddle-point electrons since the potential has no saddle points [16].

II. ION-ATOM COLLISIONS IN THE SCALED REPRESENTATION: ZERO-RANGE POTENTIALS

A. General

Consider two nuclei moving along a classical trajectory $\mathbf{R}(t)$ with the initial velocity v and impact parameter b , and one electron described by the time-dependent Schrödinger equation

$$\left[-\frac{1}{2} \nabla_{\mathbf{r}}^2 + V(\mathbf{r}, \mathbf{R}(t)) \right] \psi(\mathbf{r}, t) = i \frac{\partial \psi(\mathbf{r}, t)}{\partial t}. \quad (3)$$

This semiclassical treatment should be considered exact in a wide range of collision velocities v , with the exception of ultracold collisions. In this paper we will consider only straight-line trajectories.

The Schrödinger equation for a zero-range potential with an eigenenergy $\varepsilon_\alpha = -\alpha^2/2$ is equivalent to Eq. (3) with $V=0$ everywhere, except the point $\mathbf{r}=\mathbf{r}_{j0}$, where \mathbf{r}_{j0} is the ZRP’s position. The boundary condition determines the logarithmic derivative of the wave function $r_j \psi$ at $r_j=0$,

$$\frac{1}{r_j \psi} \left. \frac{\partial(r_j \psi)}{\partial q} \right|_{r_j \rightarrow 0} = -\alpha, \quad (4)$$

where $r_j = |\mathbf{r} - \mathbf{r}_{j0}|$. The general solution of the Schrödinger equation in the vicinity of the point $r_j = 0$ has the form

$$\psi(\mathbf{r}, t)|_{r_j \rightarrow 0} = \frac{c_j}{r_j} + b_j, \quad (5)$$

where c_j and b_j are constants. Substituting Eq. (5) into Eq. (4) we obtain the following boundary condition [15]:

$$\psi(\mathbf{r}, t)|_{r_j \rightarrow 0} = N_j(t) \left(\frac{1}{r_j} - \alpha \right), \quad (6)$$

where the coefficient $N_j(t)$ might depend on t , but not on \mathbf{r} . Systems of several ZRPs can be considered, and we attach an additional index j to distinguish positions of different ZRPs.

B. Scale transformation

The translational and rotational effects are best accounted for in scaled coordinates, as proposed by Solov'ev and Vinitsky [11]. The Solov'ev-Vinitsky scale transformation of Eqs. (3) and (6) involves the change of variables [13],

$$\mathbf{q} = \frac{\mathbf{r}}{R(t)}, \quad (7)$$

$$\tau = \int_{-\infty}^t \frac{dt'}{R^2(t')}, \quad (8)$$

and the transformation of the wave function

$$\psi(\mathbf{r}, t) = \frac{1}{R^{3/2}(\tau)} \exp\left(\frac{i\dot{R}(\tau)}{2R(\tau)} q^2\right) \varphi(\mathbf{q}, \tau). \quad (9)$$

In a reference frame that rotates counterclockwise around the vector $\mathbf{n} = \mathbf{v} \times \mathbf{b}$, where \mathbf{b} is the impact-parameter vector and \mathbf{v} is the initial-velocity vector, with the frequency Ω we obtain a new Schrödinger equation

$$\left[-\frac{1}{2} \nabla_{\mathbf{q}}^2 + \frac{1}{2} \Omega^2 q^2 + \Omega \hat{L}_n \right] \varphi(\mathbf{q}, \tau) = i \frac{\partial \varphi(\mathbf{q}, \tau)}{\partial \tau}. \quad (10)$$

In scaled coordinates $\{\mathbf{q}, \tau\}$ the ZRP's boundary conditions Eq. (6) become

$$\varphi(\mathbf{q}, \tau)|_{q_j \rightarrow 0} = N_j(\tau) \left(\frac{1}{q_j} - \alpha R(\tau) \right), \quad (11)$$

where $N_j(\tau)$ does not depend on \mathbf{q} . The Galilean invariance of $\varphi(\mathbf{q}, \tau)$ means that basis functions do not have to be modified in an *ad hoc* way by attaching the translation factors, and that they are therefore orthogonal.

The properties and advantages of the scaled transformation were presented elsewhere [13], and the reader is referred to that paper for details. Here we will only briefly summarize the most important features of this transformation. They are:

(1) In the original physical coordinates $\{\mathbf{r}, t\}$ the nuclei move along a trajectory $\mathbf{R}(t)$, therefore the interaction between the electron and the nuclei depends on the direction of the vector $\mathbf{R}(t)$. In the scaled space $\{\mathbf{q}, \tau\}$, the nuclei do not move anymore either in the radial or angular sense; they are fixed at $\mathbf{q} = \pm \hat{\mathbf{z}}/2$. Consequently, the potential in the transformed coordinates does not depend on the direction of $\mathbf{R}(t)$. The dynamical effects are described by the scalar function $R(\tau)$ and two additional terms in the new Hamiltonian of Eq. (10): the simple harmonic oscillator term and the angular momentum operator.

(2) If $|vt| \gg b$, then functions $\varphi(\mathbf{q}, \tau)$ are Galilean invariant under translations in the plane of \mathbf{v} and \mathbf{R} ; therefore *there is no need for translation factors*, i.e., phase factors that are required to write $\psi(\mathbf{r}, t)$ in frames moving relative to a particular reference frame.

(3) Since the parameter of a ZRP is changed according to $\alpha \rightarrow \alpha R(\tau)$ in scaled coordinates $\mathbf{q} = \mathbf{r}/R(t)$ [Eqs. (6) and (11)], all dependence on τ comes from the multiplicative factor $R(\tau)$ in the boundary conditions.

(4) For straight-line trajectories the nuclei rotate with the constant angular velocity $\Omega = vb$ in the scaled representation, therefore it will be convenient to introduce the angle of rotation $\theta = \Omega \tau$, $0 \leq \theta \leq \pi$, as a new "time" in the Schrödinger equation and $R(\theta) = b/\sin \theta$.

In scaled coordinates $\{\mathbf{q}, \theta\}$ the initial conditions are

$$\varphi(\mathbf{q}, \theta)|_{\theta \rightarrow 0, q_j \neq 0} = 0, \quad (12)$$

$$|\varphi(\mathbf{q}, \theta)|_{\theta \rightarrow 0, q_j / \theta = r_j / b} = |\psi_i(r_j)|. \quad (13)$$

The initial condition Eq. (12) ensures that there is no continuum in the initial state and condition Eq. (13) normalizes the wave function.

C. Electron spectra

To obtain the spectra of the ejected electrons we project our time-dependent wave function onto plane waves,

$$A(\mathbf{k}) = \lim_{t \rightarrow +\infty} \int \varphi_{\mathbf{k}}^*(\mathbf{r}, t) \psi(\mathbf{r}, t) d^3 r, \quad (14)$$

where

$$\varphi_{\mathbf{k}}(\mathbf{r}, t) = \frac{1}{(2\pi)^{3/2}} \exp\left(i\mathbf{k} \cdot \mathbf{r} - i \frac{k^2}{2} t\right). \quad (15)$$

It is more convenient to evaluate the projection in the scaled space. Since the scale transformation conserves wave-function normalization and the exponential factors cancel, one has

$$A(\mathbf{k}) = \lim_{\theta \rightarrow \pi-0} \int \varphi_{\mathbf{k}}^*(\mathbf{q}, \theta) \varphi(\mathbf{q}, \theta) d^3 q, \quad (16)$$

where the function $\varphi_{\mathbf{k}}(\mathbf{q}, \theta)$ is the transformed plane wave

$$\varphi_{\mathbf{k}}(\mathbf{q}, \theta) = \left(\frac{b}{2\pi \sin \theta} \right)^{3/2} \times \exp \left\{ \frac{i\Omega}{2 \sin \theta} \left(2 \frac{\mathbf{k}}{v} \cdot \mathbf{q} + \left[q^2 + \left(\frac{k}{v} \right)^2 \right] \cos \theta \right) \right\}. \quad (17)$$

Taking the complex conjugate and changing variables

$$\theta = \pi - \tilde{\theta}, \quad (18)$$

we have

$$\varphi_{\mathbf{k}}^*(\mathbf{q}, \theta) = \left(\frac{i}{v} \right)^{3/2} K_{\Omega}(\mathbf{q}, \tilde{\theta}; \mathbf{k}/v, 0) \xrightarrow{\tilde{\theta} \rightarrow +0} \left(\frac{i}{v} \right)^{3/2} \delta(\mathbf{q} - \mathbf{k}/v), \quad (19)$$

where K_{Ω} is the propagator for an harmonic oscillator potential with fundamental frequency Ω and the limit is obtained by definition.

Changing the order of the integration and taking the limit, we get [22]

$$A(\mathbf{k}) = \left(\frac{i}{v} \right)^{3/2} \varphi(\mathbf{q}, \theta)|_{\theta=\pi, \mathbf{q}=\mathbf{k}/v} = \left(\frac{i}{v} \right)^{3/2} \varphi(\mathbf{k}/v, \pi). \quad (20)$$

At first glance it might seem that unitarity would imply $\int |A(\mathbf{k})|^2 d\mathbf{k} = 1$, i.e., the initial state is always completely ionized. This conclusion is incorrect because one cannot interchange integration over \mathbf{k} and the limit $\theta \rightarrow \pi$.

Using COLTRIMS techniques, experimentalists measure the electron spectra at the fixed recoil momentum of the target ion. These spectra are given by the following formulas [23]:

$$T(\mathbf{k}) = \frac{iv}{(2\pi)^3} \int \exp \left[-i \int_{-\infty}^{\infty} V(b, t) dt \right] e^{-i\mathbf{K}_{\perp} \cdot \mathbf{b}} A(\mathbf{k}, \mathbf{b}) d^2b, \quad (21)$$

where \mathbf{K}_{\perp} and $K_{\parallel} = \Delta E/v$ are the components of the target-ion recoil momentum that are perpendicular and parallel to the initial velocity, respectively, and $V(b, t)$ is the atom-atom potential. In the case of the ZRP model the potential $V(b, t)$ equals zero, but to better describe the physical situation a realistic potential $V(b, t)$ could be introduced. Equation (21) represents an exact definition of $T(\mathbf{k})$ as a two-dimensional Fourier transform of $A(\mathbf{k}, \mathbf{b})$ times a phase factor. Using the stationary-phase method to evaluate the integral Eq. (21), we obtain, that $\mathbf{b} = \mathbf{b}(\mathbf{K}_{\perp})$ and

$$T(\mathbf{k}) \propto A(\mathbf{k}, \mathbf{b}(\mathbf{K}_{\perp})). \quad (22)$$

As a specific example of Eq. (22), consider a polarization potential $V(b, t) = -\alpha_0/2R^4(t)$ and ignore the phase variation of $A(\mathbf{k}, \mathbf{b})$; then

$$T(\mathbf{k}) = \frac{1}{8\pi^2} \frac{vb(K_{\perp})}{K_{\perp}} \exp \left[i \frac{2}{3} K_{\perp} b(K_{\perp}) \right] A(\mathbf{k}, \mathbf{b}(\mathbf{K}_{\perp})), \quad (23)$$

where

$$b(K_{\perp}) = \left(\frac{3\pi\alpha_0}{4vK_{\perp}} \right)^{1/4}. \quad (24)$$

In the results presented here we compute only $A(\mathbf{k}, \mathbf{b})$. Connection to a specific experiment is to be understood exactly via Eq. (21) or approximately via Eq. (24) or a variant thereof.

III. EXACT STURMIAN SOLUTION

A. Scaled representation and Sturmian functions for zero-range potentials

Since we consider only collisions of two *identical* ZRP's moving along straight-line trajectories, the time-dependent Schrödinger equation in the scaled space Eq. (10) has the form

$$\left[-\frac{1}{2} \nabla_{\mathbf{q}}^2 + \frac{1}{2} \Omega^2 q^2 + \Omega \hat{L}_n \right] \varphi(\mathbf{q}, \theta) = i\Omega \frac{\partial \varphi(\mathbf{q}, \theta)}{\partial \theta}, \quad \mathbf{q} \neq \pm \frac{\hat{\mathbf{z}}}{2}. \quad (25)$$

The boundary conditions at the ZRP's positions $\mathbf{q}_{\pm} = \pm \hat{\mathbf{z}}/2$ are

$$\varphi(\mathbf{q}, \theta)|_{|\mathbf{q}-\mathbf{q}_{\pm}| \rightarrow 0} = N_{\pm}(\theta) \left(\frac{1}{|\mathbf{q}-\mathbf{q}_{\pm}|} - \alpha R(\theta) \right), \quad (26)$$

where for straight-line trajectories

$$R(\theta) = \frac{b}{\sin \theta}. \quad (27)$$

The Sturmian functions for this problem are defined by the following differential equation

$$\left[-\frac{1}{2} \nabla_{\mathbf{q}}^2 + \frac{1}{2} \Omega^2 q^2 + \Omega \hat{L}_n \right] S_p(\omega; \mathbf{q}) = \Omega \omega S_p(\omega; \mathbf{q}), \quad (28)$$

and the boundary conditions at \mathbf{q}_{\pm} ,

$$S_p(\omega; \mathbf{q})|_{|\mathbf{q}-\mathbf{q}_{\pm}| \rightarrow 0} = \text{const} \times \left(\frac{1}{|\mathbf{q}-\mathbf{q}_{\pm}|} - \alpha \rho_p(\omega) \right), \quad (29)$$

where $\rho_p(\omega)$ are called Sturmian eigenvalues. We also require that $S_p(\omega; \mathbf{q})$ should be finite when $q \rightarrow \infty$. There are only two Sturmian functions in this case, and, since the ZRP's are identical, one of these functions is gerade, and another one is ungerade. The index p therefore will assume only two values: -1 or u and $+1$ or g . These Sturmian functions have the form [19]

$$\begin{aligned}
S_p(\omega; \mathbf{q}) &= \sqrt{\frac{\pi}{\alpha}} \left[G\left(\mathbf{q}, \frac{\hat{\mathbf{z}}}{2}, \omega\right) + p G\left(\mathbf{q}, -\frac{\hat{\mathbf{z}}}{2}, \omega\right) \right] \\
&= \frac{1}{2\sqrt{\pi\alpha} D_{\omega-1/2}(0)} \left[\frac{e^{i(v/2)\mathbf{b}\cdot\mathbf{q}}}{\left| \mathbf{q} - \frac{\hat{\mathbf{z}}}{2} \right|} \right. \\
&\quad \times D_{\omega-1/2}\left(\sqrt{2\Omega} \left| \mathbf{q} - \frac{\hat{\mathbf{z}}}{2} \right|\right) + p \frac{e^{-i(v/2)\mathbf{b}\cdot\mathbf{q}}}{\left| \mathbf{q} + \frac{\hat{\mathbf{z}}}{2} \right|} \\
&\quad \left. \times D_{\omega-1/2}\left(\sqrt{2\Omega} \left| \mathbf{q} + \frac{\hat{\mathbf{z}}}{2} \right|\right) \right], \quad (30)
\end{aligned}$$

where $G(\mathbf{q}, \mathbf{q}', \omega)$ is Green's function of the harmonic oscillator with rotation [Eq. (A11)] and $D_{\omega-1/2}(z)$ is a parabolic cylinder function [24]. These Green's functions are discussed in Appendix A. See also the paper by de Oliveira [25]. The Sturmian normalization constants $\sqrt{\pi/\alpha}$ are obtained in Appendix B from the condition

$$\int \tilde{S}_p(\omega; \mathbf{q}) S_p(\omega; \mathbf{q}) d^3q = -\frac{d\rho_p}{d\omega}, \quad (31)$$

which is equivalent to the usual Sturmian normalization condition with a potential [13] but is more convenient in the ZRP case. The dual function $\tilde{S}_p(\omega; \mathbf{q})$ is obtained from $S_p(\omega; \mathbf{q})$ by inverting the axis of rotation. Substituting Eq. (30) into Eq. (29) we obtain the Sturmian eigenvalues

$$\begin{aligned}
\rho_p(\omega) &= -\frac{1}{\alpha} \left[2\pi G_r(\omega) + p G\left(\frac{\hat{\mathbf{z}}}{2}, -\frac{\hat{\mathbf{z}}}{2}, \omega\right) \right] \\
&= -\frac{1}{\alpha} \frac{[\sqrt{2\Omega} D'_{\omega-1/2}(0) + p D_{\omega-1/2}(\sqrt{2\Omega})]}{D_{\omega-1/2}(0)}, \quad (32)
\end{aligned}$$

where $G(\mathbf{q}, \mathbf{q}', \omega)$ is Green's function of the harmonic oscillator with rotation [Eq. (A14)] and $D'_\omega(x) \equiv \partial D_\omega(x)/\partial x$.

Obviously, we can satisfy Eq. (25) by choosing solutions in the following form:

$$\varphi_p(\mathbf{q}, \theta) = \frac{1}{\sqrt{2\pi i}} \int_C B_p(\omega) S_p(\omega; \mathbf{q}) e^{-i\omega\theta} d\omega, \quad (33)$$

where C is a contour in the complex plane of ω , and $B_p(\omega)$ are the coefficients to be determined by the initial conditions Eq. (12) on $\varphi_p(\mathbf{q}, \theta)$ at $\theta \rightarrow 0$ corresponding to $t \rightarrow -\infty$.

The initial conditions depend upon the actual physical situation. In this paper we will assume two moving ZRPs infinitely far from each other with the electron either in the gerade or ungerade state as initial conditions. This choice gives two solutions $\varphi_u(\mathbf{q}, \theta)$ and $\varphi_g(\mathbf{q}, \theta)$ with well-defined symmetry. To obtain the common experimental initial condi-

tion when the electron is in the bound state of one of the ZRPs, we can combine these two functions,

$$\varphi_a(\mathbf{q}, \theta) = \frac{1}{\sqrt{2}} [\varphi_u(\mathbf{q}, \theta) + \varphi_g(\mathbf{q}, \theta)]. \quad (34)$$

The solution proceeds by satisfying the boundary conditions at ZRPs first, which leads to a three-term recurrence relation for coefficients $B_p(\omega)$. Then the solutions of the recurrence relations are chosen to ensure convergence of the integral in Eq. (33) and to satisfy the initial conditions on $\varphi_p(\mathbf{q}, \theta)$.

B. Boundary conditions and three-term recurrence relations

To satisfy the boundary conditions at ZRPs ($\mathbf{q} = \pm \hat{\mathbf{z}}/2$), we substitute the Sturmian boundary conditions Eq. (29) into the integral representation Eq. (33) and compare the result with the boundary conditions Eq. (26). We obtain the three-term recurrence relation for the coefficient $B_p(\omega)$,

$$\rho_p(\omega+1)B_p(\omega+1) - \rho_p(\omega-1)B_p(\omega-1) = 2ibB_p(\omega), \quad (35)$$

where $\rho_p(\omega)$ is the Sturmian eigenvalue given by Eq. (32).

In what follows, it will be more convenient to introduce new coefficients $C_p(\omega)$,

$$B_p(\omega) = \frac{e^{i(\pi/2)\omega}}{\rho_p(\omega)} C_p(\omega), \quad (36)$$

which satisfy the three-term recurrence relation

$$C_p(\omega+1) + C_p(\omega-1) = \frac{2b}{\rho_p(\omega)} C_p(\omega). \quad (37)$$

The asymptotic solutions of the three-term recurrence relation are derived by Braun's quasiclassical formula [26]

$$\begin{aligned}
C_p(\omega) &\approx \sqrt[4]{\frac{\rho_p^2(\omega)}{\rho_p^2(\omega) - b^2}} \\
&\quad \times \exp\left(\pm i \int_0^\omega \arcsin \frac{b}{\rho_p(\omega')} d\omega' - i \frac{\pi}{2} \omega\right), \quad (38)
\end{aligned}$$

where the Sturmian eigenvalue $\rho_p(\omega)$ is given by Eq. (32).

At large *negative* $\text{Re } \omega$ the solutions are oscillatory, and we define two linearly independent solutions $C^{L\pm}(\omega)$ by their asymptotic form Eq. (38),

$$\begin{aligned}
C^{L\pm}(\omega) &= \exp\left[\pm i \left(\frac{\pi}{2} \omega + \frac{\pi}{4} + \frac{\alpha\sqrt{2\Omega}}{v} \sqrt{-\omega}\right)\right] \\
&\quad + O(\omega^{-1/2}), \quad \text{when } \text{Re } \omega \rightarrow -\infty. \quad (39)
\end{aligned}$$

We also introduce the solutions $C^R(\omega)$ that decrease exponentially at large positive $\text{Re } \omega$:

$$C^R(\omega) = \cos\left(\frac{\pi}{2}\omega + \frac{\pi}{4}\right) \exp\left(-\frac{\alpha\sqrt{2\Omega}}{v}\sqrt{\omega}\right) + O(\omega^{-1/2}), \quad \text{when } \text{Re } \omega \rightarrow \infty. \quad (40)$$

It is important to recognize that any three-term recurrence relation has infinitely many significantly different solutions. Indeed, if we know a particular solution of a three-term recurrence relation then we can multiply this solution by an *arbitrary* periodic function with the period $T=1$ and obtain another solution of the same recurrence relation. To choose from the many solutions to the recurrence relation Eq. (37), we require that the integral in Eq. (33) must converge. The Sturmian functions $S(\omega; \mathbf{q})$ rapidly decrease at large negative $\text{Re } \omega$ on the contour C , but oscillate with slowly changing amplitude at $\text{Re } \omega > 0$. Therefore, to ensure convergence, we require that our coefficients $C_p(\omega)$ decrease at $\text{Re } \omega > 0$ on the contour C . The most general solution that decreases exponentially at large positive $\text{Re } \omega$ has a form

$$C_p(\omega) = f(\omega)C_p^R(\omega), \quad (41)$$

where $f(\omega) = f(\omega + T)$ is a periodic function with the period $T=1$.

C. Initial conditions in ω space

The initial condition Eq. (12) in ω space has the form

$$\int_C \frac{e^{i(\pi/2)\omega}}{\rho_p(\omega)} f(\omega) C_p^R(\omega) S_p(\omega; \mathbf{q}) d\omega = 0. \quad (42)$$

To satisfy the initial condition Eq. (12) we choose the contour of integration in Eq. (33) parallel to the real axis, but shifted into the complex plane by an amount $a > 0$. In this case the initial condition Eq. (12) requires that the integrand in Eq. (42) has no singularities in the upper plane and decreases exponentially on the upper semicircle at infinity. Because the Sturmian eigenvalues $\rho_p(\omega)$ have zeros and poles only on the positive real axis, this choice of the contour allows us to avoid singularities of $C^R(\omega)$ and $1/\rho_p(\omega)$ and set up the initial condition Eq. (12). Since the periodic function $f(\omega)$ should have no singularities and should not increase on the upper semicircle at infinity, then it should have the form $f(\omega) = \sum_{n=0}^{\infty} f_n e^{i2n\pi\omega}$. Notice that all terms except $n=0$ in the Fourier expansion of $f(\omega)$ give the trivial solutions $\varphi_p(\mathbf{q}, \theta) = 0$ since we can close the contour of integration in the upper plane for any θ . Then the coefficient f_0 is determined by the initial condition Eq. (13).

Our coefficients $C_p(\omega)$ should provide correct initial conditions Eq. (13) on the function $\varphi(\mathbf{q}, \theta)$. To choose the appropriate f_0 we require that for $\text{Re } \omega \rightarrow -\infty$ our calculated coefficients lead to the same stationary-phase result as the coefficients in the similar integral representation of the initial conditions. The asymptotic analysis is given in detail in Appendix C. To analyze the asymptotic behavior of $C^R(\omega)$ at large negative $\text{Re } \omega$ we write $C^R(\omega)$ as linear combination of two oscillatory solutions $C^{L\pm}(\omega)$, Eq. (39):

$$C^R(\omega) = J^+(\omega)C^{L+}(\omega) + J^-(\omega)C^{L-}(\omega). \quad (43)$$

The periodic functions $J^+(\omega)$ and $J^-(\omega)$ are determined by the Wronskians

$$J^\pm(\omega) = \mp \frac{i}{2} W\{C^R(\omega), C^{L\mp}(\omega)\}, \quad (44)$$

where $W\{A(\omega), B(\omega)\} \equiv A(\omega+1)B(\omega) - A(\omega)B(\omega+1)$. The asymptotic analysis (Appendix C) at $\theta \rightarrow 0$ and $\theta \rightarrow \pi$ by the stationary-phase method shows that

$$f_0 = 2\sqrt{2b\Omega}i[J_0^-]^{-1} \quad (45)$$

and

$$S_{00} = J_0^+[J_0^-]^{-1}, \quad (46)$$

where S_{00} is the elastic-scattering amplitude and

$$J_0^\pm = \int_0^1 J^\pm(\omega) d\omega \quad (47)$$

are the first terms in the Fourier expansions of the periodic functions $J^\pm(\omega)$. Equation (45) defines the normalization constant and the contour of integration in Eq. (33) was specified earlier. The time-dependent wave function that satisfies the initial conditions is

$$\begin{aligned} \varphi_p(\mathbf{q}, \theta) &= [J_0^-]^{-1} \sqrt{\frac{b\Omega}{\pi}} \\ &\times \int_{-\infty+ia}^{\infty+ia} e^{i\omega(\pi/2-\theta)} S_p(\omega; \mathbf{q}) \frac{C_p^R(\omega)}{\rho_p(\omega)} d\omega, \quad a > 0. \end{aligned} \quad (48)$$

An alternative Eq. (46) for the elastic scattering amplitude is

$$S_{00} = \int \varphi(\mathbf{q}, \theta) \tilde{\varphi}(\mathbf{q}, \theta) d\mathbf{q}. \quad (49)$$

Methods to evaluate Eq. (49) are discussed in Appendix D. Comparison between S_{00} from Eqs. (46) and (49) provides a check on the accuracy of our calculations.

D. Ionization probabilities and electron spectra

One way to calculate the ionization probability P_{ion} is by using unitarity

$$P_{\text{ion}} = 1 - |S_{00}|^2. \quad (50)$$

Notice that the ionization probabilities are determined only by the solutions of the three-term recurrence relations defined by Eqs. (39) and (40):

$$P_{\text{ion}} = 1 - \left| \frac{J_0^+}{J_0^-} \right|^2 = 1 - \left| \frac{\int_0^1 W\{C^R(\omega), C^{L+}(\omega)\} d\omega}{\int_0^1 W\{C^R(\omega), C^{L-}(\omega)\} d\omega} \right|^2. \quad (51)$$

To obtain electron spectra we substitute the wave function Eq. (48) into Eq. (19):

$$A(\mathbf{k}) = [J_0^-]^{-1} \frac{b}{v\sqrt{\pi i}} \int_{-\infty+ia}^{\infty+ia} e^{-i\omega\pi/2} S_p(\omega; \mathbf{k}/v) \frac{C_p^R(\omega)}{\rho_p(\omega)} d\omega. \quad (52)$$

Integrating the electron spectra over all electron momenta

$$P_{\text{ion}} = \int |A(\mathbf{k})|^2 d\mathbf{k} \quad (53)$$

is another way to calculate the ionization probability. Again, we use the two independent calculations of P_{ion} to check the accuracy of our calculations. All relevant formulas can be found in Appendix D.

E. Analytic solution for a special case

To check the method introduced above we apply it to a system with a known solution, namely, switch off one of the ZRPs. Then the exact time-dependent solution for one ZRP with parameter α moving along a straight-line trajectory $\mathbf{R}(t)$ with velocity v is

$$\Psi(\mathbf{r}, t) = \sqrt{\frac{\alpha}{2\pi}} \frac{\exp\left(-\alpha \left| \mathbf{r} - \frac{\mathbf{R}(t)}{2} \right| \right)}{\left| \mathbf{r} - \frac{\mathbf{R}(t)}{2} \right|} e^{i(\alpha^2/2)t} e^{i\mathbf{v}\cdot\mathbf{r}} e^{-i(v^2/8)t}. \quad (54)$$

In the scaled representation, Eq. (54) becomes

$$\varphi(\mathbf{q}', \theta) = \sqrt{\frac{\alpha}{2\pi}} \frac{e^{i\Omega q'_x} \sqrt{R(\theta)} \exp[-\alpha R(\theta) |\mathbf{q}' + \hat{\mathbf{z}}'/2|]}{|\mathbf{q}' + \hat{\mathbf{z}}'/2|} \times \exp\left\{-\frac{i}{2} t(\theta) [v^2 (\mathbf{q}' + \hat{\mathbf{z}}'/2)^2 - \alpha^2]\right\}, \quad (55)$$

where

$$t(\theta) = -\frac{b}{v} \cot(\theta) \quad (56)$$

and the primed coordinates remind us that we work in the rotating reference frame. We place the z axis along \mathbf{v} , the x axis along \mathbf{b} , so that the coordinate system rotates counterclockwise around y axis.

The Sturmian function for one ZRP located at $\mathbf{q} = \hat{\mathbf{z}}/2$ from Eq. (30) is

$$S(\omega; \mathbf{q}) = \frac{e^{i(\Omega/2)q_x}}{2\sqrt{\pi\alpha} |\mathbf{q} + \hat{\mathbf{z}}/2|} \frac{D_{\omega-1/2}(\sqrt{2\Omega} |\mathbf{q} + \hat{\mathbf{z}}/2|)}{D_{\omega-1/2}(0)}, \quad (57)$$

with Sturmian eigenvalues

$$\rho(\omega) = \frac{\sqrt{2\Omega} D'_{\omega-1/2}(0)}{\alpha D_{\omega-1/2}(0)} = \frac{2\sqrt{\Omega}}{\alpha} \frac{\Gamma\left(-\frac{\omega}{2} + \frac{3}{4}\right)}{\Gamma\left(-\frac{\omega}{2} + \frac{1}{4}\right)}. \quad (58)$$

The analytic solution $C^R(\omega)$ of the three-term recurrence relation Eq. (37) with $\rho(\omega)$ from Eq. (58) is found to be

$$C^R(\omega) = D'_{\omega-1/2}(0) D_{-\omega-1/2}(\sqrt{2\Omega}\alpha/v) = \cos\left(\frac{\pi}{2}\omega + \frac{\pi}{4}\right) \frac{D_{-\omega-1/2}(\sqrt{2\Omega}\alpha/v)}{D_{-\omega-1/2}(0)}, \quad (59)$$

which has the required asymptotic behavior Eq. (40) at large positive $\text{Re } \omega$. The asymptotic behavior of $C(\omega)$ at large negative $\text{Re } \omega$ is

$$C^R(\omega) \approx \cos\left(\frac{\pi}{2}\omega + \frac{\pi}{4} + \frac{\alpha\sqrt{2\Omega}}{v}\sqrt{-\omega}\right), \quad (60)$$

when $\text{Re } \omega \rightarrow -\infty$.

Comparing this with Eqs. (43) and (39) we have

$$J^\pm(\omega) = 1/2, \quad (61)$$

so that $S_{00} = 1$. This is the known result for one ZRP. To connect with Eq. (55) we substitute Eqs. (57), (58), and (59) into the integral representation Eq. (48) and compare the result with Eq. (55). In this way we obtain the following equality:

$$\begin{aligned} & \left(\frac{\alpha b}{2\pi \sin \theta}\right)^{1/2} \frac{e^{i\Omega q_x}}{\left| \mathbf{q} + \frac{\hat{\mathbf{z}}}{2} \right|} \exp\left(-\alpha b \csc \theta \left| \mathbf{q} + \frac{\hat{\mathbf{z}}}{2} \right| \right) \\ & \times \exp\left[\frac{i\Omega}{2} \cot \theta \left(\left| \mathbf{q} + \frac{\hat{\mathbf{z}}}{2} \right|^2 - \frac{\alpha^2}{v^2} \right)\right] \\ & = \frac{\sqrt{2\alpha b}}{2\pi} \frac{e^{i\Omega q_x}}{\left| \mathbf{q} + \frac{\hat{\mathbf{z}}}{2} \right|} \int_{-\infty}^{\infty} D_{-\omega-1/2}\left(\frac{\sqrt{2\Omega}\alpha}{v}\right) \\ & \times D_{\omega-1/2}\left(\sqrt{2\Omega} \left| \mathbf{q} + \frac{\hat{\mathbf{z}}}{2} \right| \right) \exp\left[i\left(\frac{\pi}{2} - \theta\right)\omega\right] d\omega. \end{aligned} \quad (62)$$

We have not found this equality in standard tables but have verified it by an asymptotic analysis. Both sides of Eq. (62) satisfy the same Schrödinger equation and asymptotic conditions, therefore the identity holds generally.

IV. COMPUTATION

To calculate $C_p^R(\omega)$ we rewrite the three-term recurrence relation Eq. (37) in the form

$$C_p^R(\omega-1) = \frac{2b}{\rho_p(\omega)} C_p^R(\omega) - C_p^R(\omega+1), \quad (63)$$

where the Sturmian eigenvalue $\rho_p(\omega)$ is given by Eq. (32). We start the solution of the three-term recurrence relation Eq. (63) at ω_i , where $\text{Re } \omega_i$ is large and positive. For example, to get the ionization probability with accuracy 10^{-7} in the case $v=1$, $b=1$, and $\alpha=1$ we use $\text{Re } \omega_i=200$. The final results should be independent of the value of $\text{Im } \omega_i > 0$, but if $\text{Im } \omega_i < 0.1$, $C_p^R(\omega)$ has very sharp structures due to poles of $1/\rho_p(\omega)$ and if $\text{Im } \omega_i > 2$, we lose accuracy since $C_p^{L+}(\omega) \ll C_p^{L-}(\omega)$. In our calculations we choose $\text{Im } \omega_i = 1$. We use the asymptotic expression Eq. (63) for the initial values $C_p^R(\omega_i)$ and $C_p^R(\omega_i+1)$.

We evaluate the recurrence relation Eq. (63) up to ω_f where we can use asymptotic expressions for $C_p^{L\pm}(\omega_f)$ given by Eq. (39) to calculate the periodic functions $J^+(\omega)$ and $J^-(\omega)$ of Eq. (44). For the same example, we use $\omega_f = 2000$. To keep requisite accuracy in the numerical evaluation of the integral in Eq. (47) we calculate $J^+(\omega)$ and $J^-(\omega)$ at 20 points from the interval $\omega_f < \omega \leq \omega_f + 1$. Then we obtain the elastic scattering amplitude S_{00} from Eq. (47).

To obtain the electron spectra

$$A(\mathbf{k}) = e^{(i/2)\mathbf{b}\cdot\mathbf{k}} a\left(\left|\frac{\mathbf{k}}{v} - \frac{\hat{\mathbf{z}}}{2}\right|\right) + p e^{-(i/2)\mathbf{b}\cdot\mathbf{k}} a\left(\left|\frac{\mathbf{k}}{v} + \frac{\hat{\mathbf{z}}}{2}\right|\right), \quad (64)$$

where

$$a(k) = \frac{b}{2\pi k v \sqrt{i\alpha} J_0^-} \int_{\omega_f}^{\omega_i} \frac{D_{\omega-1/2}(\sqrt{2\Omega}k)}{D_{\omega-1/2}(0)} \frac{C_p^R(\omega)}{\rho_p(\omega)} \times e^{-i\omega(\pi/2)} d\omega, \quad (65)$$

we substitute Sturmian functions $S_p(\omega; \mathbf{k}/v)$ from Eq. (30) to Eq. (52). Notice that Eq. (65) is singular at $k=0$. To obtain an expression free of this singularity we use the recurrence relation Eq. (63) and the recurrence relation for $D_\omega(q)/D_\omega(0)$,

$$\frac{D_{\omega+1}(q)}{D_{\omega+1}(0)} - \frac{D_{\omega-1}(q)}{D_{\omega-1}(0)} = q \frac{D_\omega(x)}{D'_\omega(0)}, \quad (66)$$

to obtain

$$a(k) = \frac{1}{2\pi v J_0^-} \sqrt{\frac{i\Omega}{2\alpha}} \int_{\omega_i}^{\omega_f} \frac{D_{\omega-1/2}(\sqrt{2\Omega}k)}{D'_{\omega-1/2}(0)} \times C_p^R(\omega) e^{-i\omega(\pi/2)} d\omega, \quad (67)$$

where

$$D'_\omega(0) = \sqrt{2\pi} \frac{2^{\omega/2}}{\Gamma(-\omega/2)} \quad (68)$$

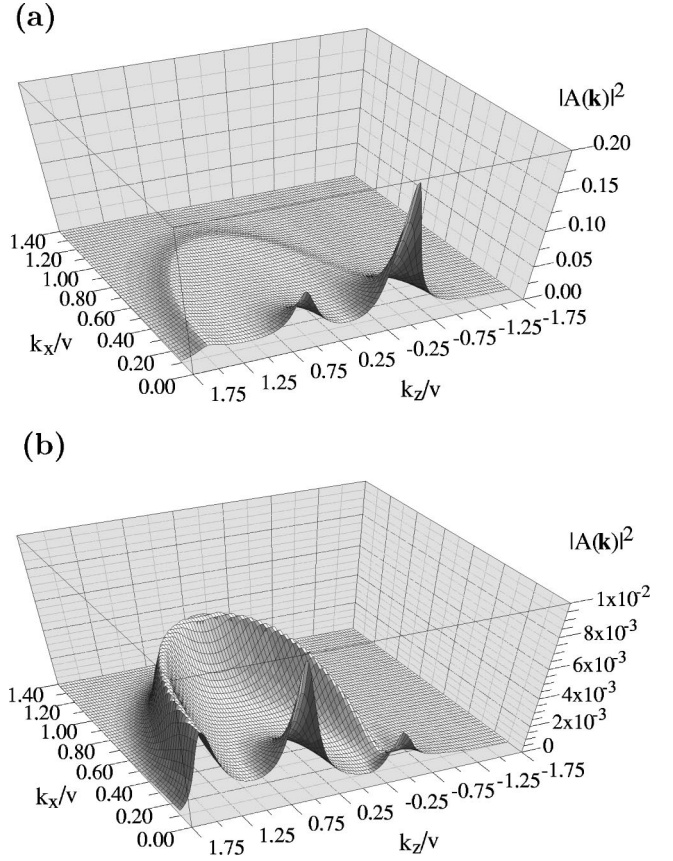


FIG. 1. Electron distributions $|A(\mathbf{k})|^2$ for the initial velocity $v = 10$ a.u. and the impact parameters $b=0.1$ a.u. (a) and $b = 0.3$ a.u. (b).

and $\Gamma(\omega)$ is the gamma function [28]. This transformation deletes singularities at $\mathbf{k}/v \pm \hat{\mathbf{z}}/2$ and removes poles in the integrand associated with zeros of $\rho_p(\omega)$.

V. RESULTS AND DISCUSSION

The computed spectrum of electrons for fast collisions, $v=10$, are shown in Fig. 1(a) for $b=0.1$ and Fig. 1(b) for $b=0.3$. Both figures contain two main features: cusps and the binary-encounter ridge. There is a prominent cusp centered at $\mathbf{k}=0$ corresponding to slow electrons in the target frame and a smaller cusp centered at $\mathbf{k}=1$ corresponding to slow electrons in the projectile frame. The binary-encounter ridge is at $|\mathbf{k}-\mathbf{v}|=v$. The relative amount of cusp electrons to binary electrons decreases rapidly with increasing impact parameter. These features are similar to those observed in high-energy ion-atom collisions. Both cusp peaks have exactly the shape predicted by and Gariabotti and Barrachina [20] for electron transfer to continuum states of neutral projectiles, namely,

$$\sigma \propto \frac{1}{Z_1^2 + |\mathbf{k}-\mathbf{v}|^2}. \quad (69)$$

The binary-encounter ridge is now no longer a pure s-wave shape, as it was for $b=0$ where we had only an

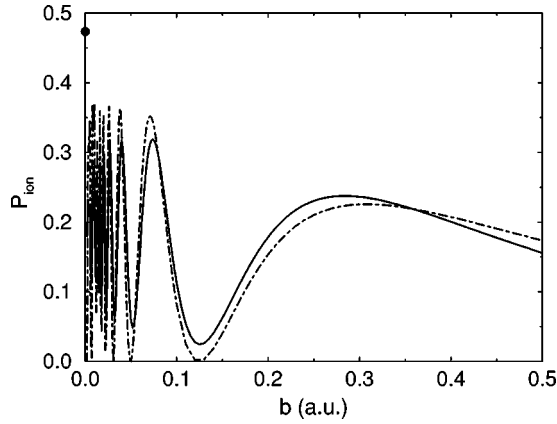


FIG. 2. The ionization probability P_{ion} as a function of the impact parameter for $v=1$ a.u. and “gerade” symmetry. The solid lines are our exact calculations and the dot-dashed lines are our two-state hidden-crossing calculations. The dot shows the result of the “zero impact parameter” calculations.

isotropic distribution in the projectile frame of reference [17]. The higher partial waves arise because rotational coupling at $b \neq 0$ transfers part of the ejected s wave to waves with $l > 0$ resulting in the departures from isotropy as seen in Fig. 1.

The results of the calculations of the ionization probabilities for initial velocity $v=1$ and gerade symmetry as a function of the impact parameter are shown in Fig. 2. The ionization cross section oscillates with increasing frequency as the impact parameter tends to zero. Figure 2 also shows the results of our calculations using the hidden-crossing theory [7]. Assuming that only one branch point is important, we have for the hidden-crossing ionization probability the result

$$P_{\text{ion}} = 4 \exp(-|S|) [1 - \exp(-|S|)] \sin^2(\Delta/2), \quad (70)$$

where

$$S = 2 \text{Im} \int_c E(\tau) d\tau, \quad \Delta = 2 \text{Re} \int_c E(\tau) d\tau, \quad (71)$$

and $E(R)$ is the adiabatic eigenenergy. The contour c starts at the point $\tau=0$ on the lowest sheet, goes around the branch

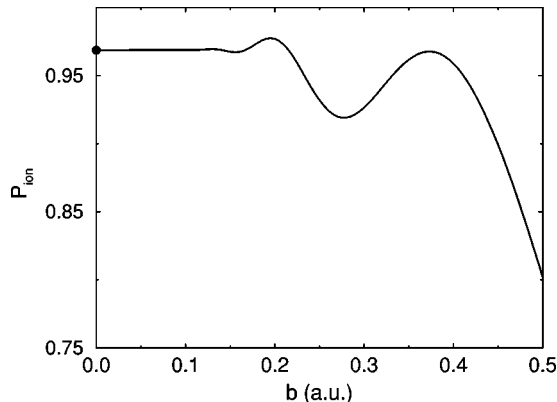


FIG. 3. The same as in Fig. 2 for “ungerade” symmetry.

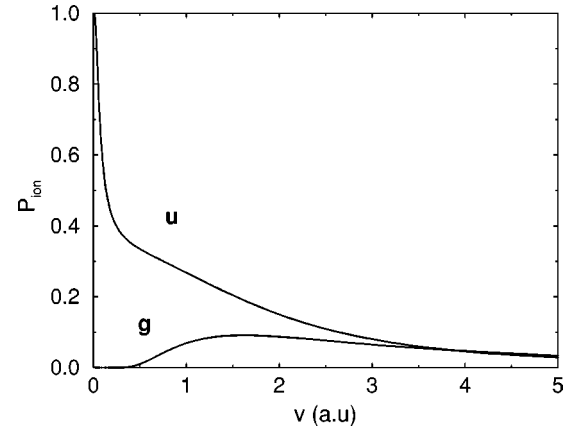


FIG. 4. The velocity dependence of the ionization probabilities P_{ion} for $b=0.8$ a.u. Probabilities corresponding to (g) “gerade” and (u) “ungerade” symmetries are shown.

point between the lowest and second sheets, and finishes at the point $\tau=0$ on the second sheet. Evaluating Eq. (71) by integrating by parts we obtain

$$\int_c E(\tau) d\tau = \int_0^\omega \arcsin \frac{b}{\rho_p(\omega')} d\omega'. \quad (72)$$

For gerade symmetry the hidden-crossing results are in good agreement with the exact calculations and show that the oscillations known as Stuekelberg oscillations are associated with the interference between the transitions of incoming and outgoing phases of collision. The hidden-crossing theory also shows that $b=0$ is an essential singularity of the ionization probability and the limit $b \rightarrow 0$ does not exist for the gerade state. Prior calculations [16] at $b=0$ give a result that is outside of the oscillations and is more than twice the average of the oscillations. For ungerade symmetry (Fig. 3) there are no oscillations, and our exact calculations uniformly reach the limit $b \rightarrow 0$ where they coincide with prior calculations [16] at $b=0$.

The velocity dependence of the ionization probabilities for $b=0.8$ are shown in Fig. 4. While for high velocities the ionization probabilities are approximately the same, for low

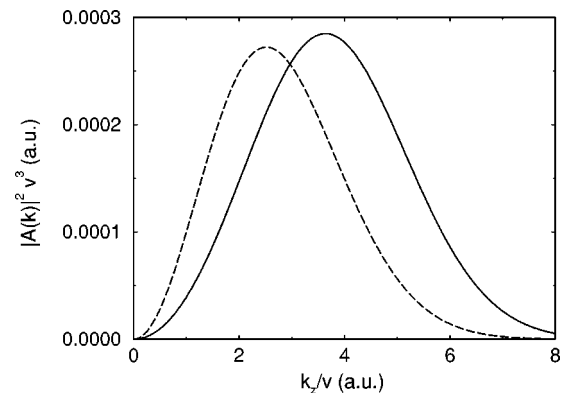


FIG. 5. Comparison of exact, solid curve, and two-state hidden crossing, dot-dashed, electron distributions $|A(\mathbf{k})|^2 v^3$ vs k_z/v for $v=0.2$ a.u., $b=0.8$ a.u. in the center-of-mass frame.

velocities the ionization probability for ungerade symmetry is much greater than that for gerade symmetry. For this reason we do not find Fermi oscillations in the electron spectra.

Figure 5 shows the comparison between the exact calculations of the electron spectra for $b=0.8$, $v=0.2$, and the two-state hidden-crossing calculations [27] in the case of ungerade symmetry. The total ionization probability is 3.5 times bigger than the two-state hidden-crossing result suggesting that more adiabatic states are involved in the ionization process.

Additional results not directly connected with the main topic of the manuscript are the simplified expression of the harmonic-oscillator Green's function [19,25] given in Appendix A and the integral Eq. (62) that we cannot find in tables of integrals. This result is written generally as

$$\int_{-\infty}^{\infty} D_x(a)D_{-x-1}(b)e^{ic(x-1/2)}dx = \sqrt{\frac{\pi}{\cos c}} \exp\left[\frac{i}{4}(a^2-b^2)\tan c - \frac{ab}{2\cos c}\right]. \quad (73)$$

VI. CONCLUSIONS

We have developed new mathematical techniques that provide the first semianalytical solution of a nontrivial model for ion-atom collisions at impact parameters not equal to zero. These new techniques involve mainly finding appropriate integration contours and solutions of three-term recurrence relations, such that physical boundary and initial conditions are satisfied. While the mathematics needed to verify the techniques are fairly involved, the computational procedure is actually quite simple. This method can serve to guide similar approaches to other physical systems. In addition, our numerical results can be used to benchmark alternative computational methods. To that end we have presented complete electron momentum distributions at select velocities and impact parameters.

A comparison with the hidden-crossing theory at low velocities shows good agreement for the gerade symmetry, but only order-of-magnitude agreement for the ungerade symmetry. It appears that more adiabatic states must be considered in this latter case. Our results could serve as simulation data for further tests of the hidden-crossing method for $b \neq 0$.

It may even be possible to test some of the predictions experimentally. The cusps and binary ridge at high velocities are expected, but our new results show that the ridge is anisotropic even though electron ejection occurs only via s -wave scattering. At low energies, the absence of Fermi oscillations in the electron spectra is the main new feature. This absence is traced to the small value of the gerade amplitudes.

ACKNOWLEDGMENTS

This research is sponsored by the Division of Chemical Sciences, Office of Basic Energy Sciences, U.S. Department of Energy, under Contract No. DE-AC05-00OR22725 with UT-Battell, LLC.

APPENDIX A: GREEN'S FUNCTIONS

We find the Green's functions from the expression

$$G(\mathbf{q}', \mathbf{q}'', E) = \int_0^{\infty} K(\mathbf{q}', \mathbf{q}'', -it)e^{-Et} dt, \quad (A1)$$

where $K(\mathbf{q}', \mathbf{q}'', t)$ is a propagator. The propagator $K(\mathbf{q}', \mathbf{q}'', t)$ is a periodic function with period T_0 and has singularities at integral multiples of T_0 .

1. One-dimensional harmonic oscillator

The propagator $K(q_1, q_2, t)$ and Green's functions $G(q_1, q_2, E)$ for one-dimensional harmonic oscillator has the form

$$K^{1D}(q_1, q_2, t) = \left(\frac{\Omega}{2\pi i \sin \Omega t}\right)^{1/2} \times \exp\left[\frac{i\Omega}{2 \sin \Omega t}[(q_1^2 + q_2^2)\cos \Omega t - 2q_1 q_2]\right], \quad (A2)$$

$$G^{1D}(q_1, q_2, E) = \frac{2}{\sqrt{\pi\Omega}} \Gamma(1/2 - E/\Omega) D_{E/\Omega - 1/2}(\sqrt{2\Omega} q_>) \times D_{E/\Omega - 1/2}(-\sqrt{2\Omega} q_<). \quad (A3)$$

2. Three-dimensional harmonic oscillator

The propagator $K(\mathbf{q}', \mathbf{q}'', t)$ and Green's functions $G(\mathbf{q}', \mathbf{q}'', E)$ for three-dimensional harmonic oscillator has the form

$$K(\mathbf{q}', \mathbf{q}'', t) = \left(\frac{\Omega}{2\pi i \sin \Omega t}\right)^{3/2} \exp\left[\frac{i\Omega}{2 \sin \Omega t}[(q'^2 + q''^2) \times \cos \Omega t - 2\mathbf{q}' \cdot \mathbf{q}'']\right], \quad (A4)$$

$$G(\mathbf{q}', \mathbf{q}'', E) = \frac{\Gamma(1/2 - E/\Omega)}{2\pi\sqrt{\pi\Omega}|\mathbf{q}' - \mathbf{q}''||\mathbf{q}' + \mathbf{q}''|} \times \left[q_< \frac{\partial}{\partial q_>} - q_> \frac{\partial}{\partial q_<}\right] \times D_{E/\Omega - 1/2}(\sqrt{2\Omega} q_>) D_{E/\Omega - 1/2}(-\sqrt{2\Omega} q_<). \quad (A5)$$

3. Three-dimensional harmonic oscillator with rotation

The propagator $K(\mathbf{q}', \mathbf{q}'', t)$ and Green's functions $G(\mathbf{q}', \mathbf{q}'', E)$ for three-dimensional harmonic oscillator with rotation has the form

$$K_{\text{rot}}(\mathbf{q}', \mathbf{q}'', t) = \left(\frac{\Omega}{2\pi i \sin \Omega t} \right)^{3/2} \exp(i[\mathbf{q}' \times \boldsymbol{\Omega}] \cdot \mathbf{q}'') \times \exp \left[\frac{i\Omega}{2 \sin \Omega t} [(|\mathbf{q}' - \mathbf{q}''|^2 + 2y'y'')] \right] \times \cos \Omega t - 2y'y'' \Big], \quad (\text{A6})$$

$$G_{\text{rot}}(\mathbf{q}', \mathbf{q}'', E) = \frac{\exp(i[\mathbf{q}' \times \boldsymbol{\Omega}] \cdot \mathbf{q}'')}{2\pi |\mathbf{q}' - \mathbf{q}''| |\mathbf{q}' - \mathbf{q}_{xz}''|} \frac{\Gamma(1/2 - E/\Omega)}{\sqrt{\pi\Omega}} \times \left[\eta \frac{\partial}{\partial \xi} - \xi \frac{\partial}{\partial \eta} \right] D_{E/\Omega - 1/2}(\sqrt{2\Omega}\xi) \times D_{E/\Omega - 1/2}(-\sqrt{2\Omega}\eta), \quad (\text{A7})$$

where

$$\xi = \frac{1}{2} (|\mathbf{q}' - \mathbf{q}''| + |\mathbf{q}' - \mathbf{q}_{xz}''|),$$

$$\eta = \frac{1}{2} (|\mathbf{q}' - \mathbf{q}''| - |\mathbf{q}' - \mathbf{q}_{xz}''|) = y'y''/\xi,$$

$$|\mathbf{q}' - \mathbf{q}_{xz}''| = \sqrt{|\mathbf{q}' - \mathbf{q}''|^2 + 4y'y''}, \quad (\text{A8})$$

$\mathbf{q}_{xz} = (x, -y, z)$ is the reflection of \mathbf{q} in xz plane. In terms of Whittaker functions [25] the Green's function has the form

$$G_{\text{rot}}(\mathbf{q}', \mathbf{q}'', E) = \frac{\exp(i[\mathbf{q}' \times \boldsymbol{\Omega}] \cdot \mathbf{q}'')}{4\pi^{3/2} |\mathbf{q}' - \mathbf{q}''| |\mathbf{q}' - \mathbf{q}_{xz}''|} \left[\eta \frac{\partial}{\partial \xi} - \xi \frac{\partial}{\partial \eta} \right] \times \left[2\Gamma\left(\frac{3}{4} - \frac{E}{2\Omega}\right) M_{E/2\Omega, 1/4}(\Omega\xi^2) \times W_{E/2\Omega, 1/4}(\Omega\eta^2) + \Gamma\left(\frac{1}{4} - \frac{E}{2\Omega}\right) M_{E/2\Omega, -1/4}(\Omega\xi^2) \times W_{E/2\Omega, -1/4}(\Omega\eta^2) \right]. \quad (\text{A9})$$

For $y=0$ we have

$$K_{\text{rot}}(\mathbf{q}', \mathbf{q}'', t) = \left(\frac{\Omega}{2\pi i \sin \Omega t} \right)^{3/2} \exp(i[\mathbf{q}' \times \boldsymbol{\Omega}] \cdot \mathbf{q}'') \times \exp \left(\frac{i\Omega}{2} |\mathbf{q}' - \mathbf{q}''|^2 \cot \Omega t \right), \quad (\text{A10})$$

and

$$G_{\text{rot}}(\mathbf{q}', \mathbf{q}'', E) = \frac{\exp(i[\mathbf{q}' \times \boldsymbol{\Omega}] \cdot \mathbf{q}'')}{2\pi |\mathbf{q}' - \mathbf{q}''|} \frac{D_{E/\Omega - 1/2}(\sqrt{2\Omega}|\mathbf{q}' - \mathbf{q}''|)}{D_{E/\Omega - 1/2}(0)}. \quad (\text{A11})$$

4. Regularized Green's functions

Regularized Green's functions are defined as

$$G_r(\mathbf{q}, E) = \lim_{\mathbf{q} \rightarrow \mathbf{q}'} \left[G(\mathbf{q}, \mathbf{q}', E) - \frac{1}{2\pi |\mathbf{q} - \mathbf{q}'|} \right]. \quad (\text{A12})$$

The Green's functions $G_r(\mathbf{q}, E)$ for 3D oscillator with rotation has the form

$$G_r(\mathbf{q}, E) = \frac{1}{(2\pi)^{3/2}} \frac{1}{2\sqrt{2\Omega}} \Gamma\left(\frac{1}{2} - \frac{E}{\Omega}\right) \left[\frac{1}{y} \frac{\partial}{\partial y} - \frac{\partial^2}{\partial q^2} \right] \times D_{E/\Omega - 1/2}[\sqrt{2\Omega}(y+q)] \times D_{E/\Omega - 1/2}[-\sqrt{2\Omega}(y-q)]|_{q=0}. \quad (\text{A13})$$

For $y=0$ we have

$$G_r(E) = \frac{\sqrt{2\Omega}}{2\pi} \frac{D'_{E/\Omega - 1/2}(0)}{D_{E/\Omega - 1/2}(0)}. \quad (\text{A14})$$

APPENDIX B: NORMALIZATION INTEGRALS

To normalize Sturmian functions we calculate the integral

$$\int \tilde{S}_p(\omega; \mathbf{q}) S_p(\omega; \mathbf{q}) d^3q = N^2 \left[\int \tilde{G}\left(\mathbf{q}, \frac{\hat{\mathbf{z}}}{2}, \omega\right) G\left(\mathbf{q}, \frac{\hat{\mathbf{z}}}{2}, \omega\right) d^3q + \int \tilde{G}\left(\mathbf{q}, -\frac{\hat{\mathbf{z}}}{2}, \omega\right) G\left(\mathbf{q}, -\frac{\hat{\mathbf{z}}}{2}, \omega\right) d^3q + p \int \tilde{G}\left(\mathbf{q}, \frac{\hat{\mathbf{z}}}{2}, \omega\right) G\left(\mathbf{q}, -\frac{\hat{\mathbf{z}}}{2}, \omega\right) d^3q + p \int \tilde{G}\left(\mathbf{q}, -\frac{\hat{\mathbf{z}}}{2}, \omega\right) G\left(\mathbf{q}, \frac{\hat{\mathbf{z}}}{2}, \omega\right) d^3q \right], \quad (\text{B1})$$

where tildes over letters indicate dual functions obtained by reversing the direction of the rotation axis. To calculate the integrals in Eq. (B1) we use the relation

$$\int \tilde{G}(\mathbf{q}, \mathbf{q}', \omega) G(\mathbf{q}, \mathbf{q}'', \omega) d^3q = \frac{\partial}{\partial \omega} G(\mathbf{q}', \mathbf{q}'', \omega), \quad (\text{B2})$$

and the explicit form of the Green's function (A11). The final result is

$$\int \tilde{S}_p(\omega; \mathbf{q}) S_p(\omega; \mathbf{q}) d^3q = -N^2 \frac{\alpha}{\pi} \frac{d\rho_p}{d\omega}, \quad (\text{B3})$$

then

$$N = \sqrt{\frac{\pi}{\alpha}}, \quad (\text{B4})$$

and the properly normalized Sturmian functions are

$$S_p(\omega; \mathbf{q}) = \sqrt{\frac{\pi}{\alpha}} \left[G\left(\mathbf{q}, \frac{\hat{\mathbf{z}}}{2}, \omega\right) + p G\left(\mathbf{q}, -\frac{\hat{\mathbf{z}}}{2}, \omega\right) \right]. \quad (\text{B5})$$

APPENDIX C: ASYMPTOTIC ANALYSIS

To see the connection between the ω space and θ space we calculate integral in Eq. (33) by the stationary-phase method. We assume that only large negative $\text{Re } \omega$ will contribute to the integral when $\theta \rightarrow 0$. We use the asymptotic formula Eq. (39) for parabolic cylinder functions with $\text{Re } a \rightarrow -\infty$. Then the phase to examine is

$$\phi(\omega) = -\frac{\pi}{4} - \omega\theta - y\sqrt{-\omega}, \quad (\text{C1})$$

where

$$y = \sqrt{2\Omega}(\alpha/v - iq), \quad q = |\mathbf{q}' + \hat{\mathbf{z}}|. \quad (\text{C2})$$

By differentiating Eq. (C1) with respect to ω , we find the stationary-phase point

$$\sqrt{-\omega_0} = \frac{y}{2\theta}, \quad (\text{C3})$$

the second derivative at the stationary point

$$\phi''(\omega_0) = -\frac{\theta}{2\omega_0}, \quad (\text{C4})$$

and the value of the stationary phase

$$\phi(\omega_0) = \theta\omega_0 - \frac{\pi}{4}. \quad (\text{C5})$$

We should note here that the imaginary part of the stationary point ω_0 given by Eq. (C3) is always positive. In order to be consistent with our assumption that only large negative $\text{Re } \omega$ contribute to the integral Eq. (33), we must require

$$q < \alpha/v \quad (\text{C6})$$

in these formulas.

We apply stationary-phase formula

$$\int f(\omega) \exp[i\phi(\omega)] d\omega \approx \sqrt{\frac{2\pi i}{\phi''(\omega_0)}} f(\omega_0) \exp[i\phi(\omega_0)], \quad (\text{C7})$$

to get

$$\varphi^-(q, \theta) \approx \sqrt{\frac{\alpha b}{2\pi\theta}} \frac{e^{i\Omega q_x}}{q} \exp\left[-i\frac{vb}{2\theta}(\alpha/v - iq)^2\right], \quad (\text{C8})$$

which is exactly the asymptotic form of Eq. (55) for $\theta \rightarrow 0$.

Let us consider the contribution from the other part of cosine (positive imaginary exponent). With the same assumptions as before the phase becomes

$$\phi^+(\omega) = (\pi - \theta)\omega + \frac{\pi}{4} + y^* \sqrt{-\omega}, \quad (\text{C9})$$

and the stationary point is

$$\sqrt{-\omega_0^+} = -\frac{y^*}{2(\pi - \theta)}. \quad (\text{C10})$$

The second derivative at the stationary point is

$$\phi''(\omega_0^+) = -\frac{\pi - \theta}{2\omega_0^+}, \quad (\text{C11})$$

and the phase at the stationary point is

$$\phi(\omega_0^+) = \frac{\pi}{4} - (\pi - \theta)\omega_0^+. \quad (\text{C12})$$

The stationary point for this term always lies in the lower half-plane of ω . Again, to satisfy the additional condition (C6) the real part of ω_0^+ is taken to be negative. Assuming that all conditions are satisfied we obtain

$$\begin{aligned} \varphi^+(q, \theta) \approx & i \sqrt{\frac{\alpha b}{2\pi(\pi - \theta)}} \frac{e^{i\Omega q_x}}{q} \\ & \times \exp\left[i\frac{vb}{2(\pi - \theta)}(\alpha/v + iq)^2\right], \quad (\text{C13}) \end{aligned}$$

which differs only by a factor of i from the asymptotic form of Eq. (55) for $\theta \rightarrow \pi - 0$.

Thus, we see that behavior of the solution at $\theta \rightarrow 0$ and $\theta \rightarrow \pi - 0$ is determined by stationary-phase points at large negative $\text{Re } \omega$. This fact is used to set up initial conditions in the problem with two ZRPs.

APPENDIX D: NORMALIZATION OF TIME-DEPENDENT SOLUTIONS

The exact time-dependent solution can be written as

$$\begin{aligned} \varphi(\mathbf{q}, \theta) = & \frac{\exp[-i(\Omega/2)q_r \cos \phi]}{q_+} F_p(q_+, \theta) \\ & + p \frac{\exp[i(\Omega/2)q_r \cos \phi]}{q_-} F_p(q_-, \theta), \quad (\text{D1}) \end{aligned}$$

where

$$F_p(k, \theta) = \frac{1}{2\pi J_0} \sqrt{\frac{b\Omega}{\alpha}} \times \int_{-\infty+ia}^{\infty+ia} e^{i\omega(\pi/2-\theta)} \frac{D_{\omega-1/2}(\sqrt{2\Omega}k)}{D_{\omega-1/2}(0)} \frac{C_p^R(\omega)}{\rho_p(\omega)} d\omega, \quad (D2)$$

$$a > 0, \quad (D2)$$

$$q_{\pm} = \sqrt{q_r^2 + (q_z \pm 1/2)^2}, \quad (D3)$$

and q_r , q_z , and θ are the cylindrical coordinates of \mathbf{q} . We want to calculate the normalization integral

$$N(\theta) = \int |\varphi(\mathbf{q}, \theta)|^2 d\mathbf{q}. \quad (D4)$$

Using Eq. (D1) we write

$$|\varphi(\mathbf{q}, \theta)|^2 = I_1(q_+, \theta) + I_1(q_-, \theta) + pI_2(\mathbf{q}, \theta), \quad (D5)$$

where

$$I_1(q_{\pm}, \theta) = \frac{|F_p(q_{\pm}, \theta)|^2}{q_{\pm}^2},$$

$$I_2(\mathbf{q}, \theta) = \frac{2}{q_+q_-} \text{Re}[e^{-i\Omega q_r \cos \phi} F_p(q_+, \theta) F_p^*(q_-, \theta)]. \quad (D6)$$

It is easy to show that

$$\int I_1(q_{\pm}, \theta) d^3q = 4\pi \int_0^{\infty} |F_p(q, \theta)|^2 dq. \quad (D7)$$

In the last term we use the integral representation of a Bessel function [28],

$$J_0(z) = \frac{1}{2\pi} \int_0^{2\pi} e^{\pm iz \cos \phi} d\phi \quad (D8)$$

to get

$$\int_0^{2\pi} I_2(\mathbf{q}, \theta) d\phi = 4\pi \frac{J_0(q_r \Omega)}{q_+q_-} \text{Re}[F_p(q_+, \theta) F_p^*(q_-, \theta)]. \quad (D9)$$

It is convenient to use elliptic coordinates in further integrations

$$\xi = q_+ + q_-,$$

$$\eta = q_+ - q_-. \quad (D10)$$

We now have for the volume integral

$$\int_0^{2\pi} I_2(\mathbf{q}, \theta) d\mathbf{q} = 2\pi \int_0^{\infty} \int_{-1}^1 J_0[\Omega \sqrt{(\xi^2-1)(1-\eta^2)}/2] \times \text{Re}\{F_p[(\xi+\eta)/2, \theta] F_p^*[(\xi-\eta)/2, \theta]\} d\xi d\eta. \quad (D11)$$

The final result is

$$N(\theta) = 8\pi \int_0^{\infty} |F_p(q, \theta)|^2 dq + 2\pi \int_0^{\infty} \int_{-1}^1 J_0[\Omega \sqrt{(\xi^2-1)(1-\eta^2)}/2] \times \text{Re}\{F_p[(\xi+\eta)/2, \theta] F_p^*[(\xi-\eta)/2, \theta]\} d\xi d\eta. \quad (D12)$$

We evaluate this integral numerically to check that $N(\theta) = 1$ for $0 < \theta < \pi$, $N(0) = 0$, and $P_{\text{ion}} = N(\pi)$.

To check the accuracy of our calculations of the elastic scattering amplitude S_{00} we use the following formulas:

$$S_{00} = \int \varphi(\mathbf{q}, \theta) \tilde{\varphi}(\mathbf{q}, \theta) d\mathbf{q}. \quad (D13)$$

Using the same technique we obtain

$$S_{00} = 8\pi \int_0^{\infty} F_p^2(q, \theta) dq + 2\pi \int_0^{\infty} \int_{-1}^1 J_0[\Omega \sqrt{(\xi^2-1)(1-\eta^2)}/2] \times F_p[(\xi+\eta)/2, \theta] F_p[(\xi-\eta)/2, \theta] d\xi d\eta. \quad (D14)$$

The integral is evaluated numerically.

- [1] R. Dörner *et al.*, Phys. Rev. Lett. **77**, 4520 (1996).
 [2] E.Y. Sidky and C.D. Lin, J. Phys. B **31**, 2949 (1998); Phys. Rev. A **60**, 377 (1999).
 [3] J.C. Wells, D.R. Schultz, P. Gavras, and M.S. Pindzola, Phys. Rev. A **54**, 593 (1996).
 [4] D.R. Schultz, M.R. Strayer, and J.C. Wells, Phys. Rev. Lett. **82**, 3976 (1999).
 [5] T.G. Winter, Phys. Rev. A **37**, 4656 (1988).
 [6] R. Shingal and C.D. Lin, J. Phys. B **22**, L445 (1989).

- [7] S.Y. Ovchinnikov and E.A. Solov'ev, Comments At. Mol. Phys. **22**, 69 (1988).
 [8] W. Fritsch and C.D. Lin, Phys. Rev. A **26**, 762 (1982); **27**, 3361 (1983).
 [9] D.R. Bates and R. McCarroll, Proc. R. Soc. London, Ser. A **245**, 175 (1958).
 [10] R. McCarroll and D.S.F. Crothers, Adv. At., Mol., Opt. Phys. **32**, 253 (1994).
 [11] E.A. Solov'ev and S.I. Vinitzky, J. Phys. B **18**, L557 (1985).

- [12] E.A. Solov'ev, Usp. Fiz. Nauk. **157**, 437 (1989) [Sov. Phys. Usp. **32**, 228 (1989)].
- [13] S.Y. Ovchinnikov, J.H. Macek, and D.B. Khrebtukov, Phys. Rev. A **56**, 2872 (1997).
- [14] S.Y. Ovchinnikov and J.H. Macek, Phys. Rev. Lett. **75**, 2474 (1995).
- [15] Yu.N. Demkov and V.N. Ostrovskii, *Metod Potentsialov Nulevogo Radiusa v Atomnoi Fizike*. English translation: *Zero-range Potentials and Their Application in Atomic Physics*, translated from Russian by A.M. Ermolaev (Plenum Press, New York, 1988), p. 5.
- [16] M.J. Rakovic and E.A. Solov'ev, Phys. Rev. A **41**, 3635 (1990).
- [17] J.H. Macek, S.Y. Ovchinnikov, and E.A. Solov'ev, Phys. Rev. A **60**, 1140 (1999).
- [18] J.H. Macek and M.J. Cavagnero, Phys. Rev. A **58**, 348 (1998).
- [19] D.B. Khrebtukov and J.H. Macek, J. Phys. A **31**, 2853 (1998).
- [20] C.R. Garibotti and R.O. Barrachina, Phys. Rev. A **28**, 2792 (1983); R.O. Barrachina, J. Phys. B **23**, 3221 (1990).
- [21] J. Wang, J. Burgdörfer, and A. Bány, Phys. Rev. A **43**, 4036 (1991).
- [22] J.H. Macek and S.Y. Ovchinnikov, Phys. Rev. Lett. **80**, 2298 (1998).
- [23] J.H. Macek and J. Briggs, Adv. At., Mol., Opt. Phys. **28**, 1 (1991).
- [24] I.S. Gradshteyn and I.M. Ryzhik, *Tables of Integrals, Series, and Products* (Academic Press, New York, 1965), pp. 1064ff.
- [25] E. Capelas de Oliveira, Rev. Bras. Fis. **9**, 697 (1979).
- [26] P.A. Braun, Rev. Mod. Phys. **65**, 115 (1993).
- [27] T. Grozdanov and E.A. Solov'ev, Eur. Phys. J. D **6**, 13 (1999).
- [28] M. Abramowitz and I.A. Stegun, *Handbook of Mathematical Formulas* (Dover, New York, 1972), pp. 255ff and 360ff.